Optical matrix elements in tight-binding models with overlap

Titus Sandu*
Department of Chemical and Materials Engineering, Arizona State University, Tempe, Arizona 85287-6006, USA
(Received 26 May 2005; revised manuscript received 27 June 2005; published 7 September 2005;
publisher error corrected 12 September 2005)

We investigate the effect of orbital overlap on optical matrix elements in empirical tight-binding models. Empirical tight-binding models assume an orthogonal basis of (atomiclike) states and a diagonal coordinate operator which neglects the intra-atomic part. It is shown that, starting with an atomic basis which is not orthogonal, the orthogonalization process induces intra-atomic matrix elements of the coordinate operator and extends the range of the effective Hamiltonian. We analyze simple tight-binding models and show that nonorthogonality plays an important role in optical matrix elements. In addition, the procedure gives formal justification to the nearest-neighbor spin-orbit interaction introduced by Boykin [Phys. Rev. B **57**, 1620 (1998)] in order to describe the Dresselhaus term which is neglected in empirical tight-binding models.

DOI: 10.1103/PhysRevB.72.125105 PACS number(s): 78.20.−e, 71.15.−m, 78.67.−n, 73.22.−f

I. INTRODUCTION

The tight-binding (TB) approach to electronic structure is one of the most used methods in solid state systems.[1] The empirical tight-binding (ETB) method, which dates back to the work of Slater and Koster,[2] assumes mostly two-center approximation and the matrix elements of the Hamiltonian between orthogonal and atom-centered orbitals[3] are treated as parameters fitted to experiment or first-principles calculations. ETB is widely employed to the description of electronic structure of complex systems[4] like interfaces and defects in crystals, amorphous materials, nanoclusters, and quantum dots because it is computationally efficient (up to three orders of magnitude faster than the *ab initio* density functional methods) and provides physically transparent results. Many calculations consider just the nearest-neighbor Hamiltonian with fewer parameters but with additional orbitals introduced.[5] To consider a higher accuracy, the range of the Hamiltonian is extended to few nearest-neighbor shells (up to the first three shells) and, therefore more fitting parameters.[6] However, the use of a nonorthogonal formalism might scale back the range of the Hamiltonian having the additional fitting from the overlap matrix. In some instances,[7] when strain is present, nonorthogonality is invoked implicitly to accommodate the changes of the on-site energies due to local displacements in addition to the well known scaling of the transfer integrals.[8] A nonorthogonal formalism has also a less obvious advantage. Because they have a longer range than the atomic orbitals, the orthogonalized orbitals samples the local environment, making them better suited for transferability to complex systems.[9]

Calculation of optical spectra in the ETB formalism requires the knowledge of additional parameters: the momentum or velocity matrix elements between initial and final states. In the early work, momentum matrix elements were considered as extra parameters fitted to the experimental or first-principles calculated dielectric function. However, ETB has been extended to include the interaction with electromagnetic fields[10] by making the substitution $p=(m_0/\hbar)\nabla_k H$, such that dielectric function and other optical properties can be calculated without additional parameters. The scheme is based on the Peierls substitution of Hamiltonian matrix elements[11] allowing us to calculate directly the momentum or velocity matrix elements. In Refs. 12 and 13 it is shown that the substitution $p=(m_0/\hbar)\nabla_k H$ leads to the neglect of the intra-atomic momentum matrix elements or, equivalently, the coordinate operator is diagonal in the subsequent basis as we will indicate below. However, the Peierls-tight-binding (i.e., zero intra-atomic position parameters) has been successfully used in Ref. 14. Pedersen *et al.*[13] introduced an additional momentum matrix element to accommodate the intra-atomic transitions. In contrast, Boykin and Vogl[15] showed that adding intra-atomic terms suppresses the gauge invariance. To circumvent this problem Foreman[16] used group theory arguments to construct the basis in which intra-atomic matrix elements are present and the lattice gauge theory to define the interaction of electromagnetic fields with electrons in crystals.

The effect of orbital overlapping on electronic structure has been studied for simple systems.[17,18] In this paper we investigate the optical matrix elements in the presence of nonorthogonal (overlapping) orbitals. As far as we know, no study has been done in this direction. We show that intra-atomic contributions of the coordinate operator are induced simply by the orthogonalization process. The orthogonalization process induces terms equivalent with more distant interactions, such that it gives formal justification for the nearest-neighbor spin-orbit interaction introduced in Ref. 19 for the TB model with spin-orbit interaction.[20] The analysis of simple systems shows that the nonorthogonal orbitals play an important role on optical matrix elements. We reanalyze the example of Pedersen *et al.*[13] to show that the nonorthogonal orbitals improve the optical matrix elements. In the case of graphene, the overlap and TB parametrization are crucial in explaining the experimental data. Moreover, similar arguments can be employed in the *ab initio* tight binding linear muffin-tin orbitals (TB-LMTO) method,[21] leading to faster calculations of optical matrix elements in a parameter free theory.

II. TIGHT-BINDING CALCULATIONS AND NONORTHOGONALITY

To fix ideas we consider a localized basis $|\alpha R)$, where α is the orbital type and R is the center of the orbital (Löwdin orbitals).[3] The crystal Hamiltonian H is diagonalized within the Bloch sums of the localized basis

$$|\alpha k) = 1/\sqrt{N}\sum_R e^{ikR}|\alpha R) \tag{1}$$

as follows:

$$|nk\rangle = \sum_\alpha c_{n\alpha}(k)|\alpha k), \tag{2}$$

with

$$H(k)|nk\rangle = E_{nk}|nk\rangle. \tag{3}$$

The kinematic momentum operator involved in optical transitions is defined as

$$p = \frac{m}{i\hbar}[r,H]. \tag{4}$$

In the crystal momentum representation,[22] the kinematic momentum operator is

$$p = \frac{m}{\hbar}\nabla_k H(k), \tag{5}$$

where $H(k)$ is the Hamiltonian in the crystal momentum representation. Equation (5) holds in a complete basis as well as in an incomplete basis. However, in an incomplete basis the momentum operator p and coordinate operator r do not satisfy the canonical commutation relations leading to different formula for effective masses and Peierls-coupling formula involving the vector potential. These issues are detailed in Refs. 23 and 24. The coordinate operator r is considered to have the following matrix elements in the localized basis $|\alpha R)$:

$$(\alpha' R'|r|\alpha R) = (R\delta_{\alpha\alpha'} + d_{\alpha\alpha'})\delta_{RR'}, \tag{6}$$

since the overlapping of the orbitals belonging to different atoms is supposed to be small. Here $d_{\alpha\alpha'}$ is the intra-atomic matrix element. In the usual tight-binding theory the coordinate operator is diagonal.[10] Therefore the intra-atomic parts are neglected[12,13] leading to no need of other fitting parameters beyond those of the Hamiltonian and to gauge invariance.

Pedersen *et al.*[13] pointed out that there are cases in which the neglect of the intra-atomic part may conduct to the underestimation of the momentum operator arguing that by using Eqs. (1)–(4),

$$\langle nk|p|mk\rangle = \frac{im}{\hbar}\sum_{\alpha,\alpha'} c^*_{n\alpha'}(k)c_{m\alpha}(k)\nabla_k(\alpha' k|H|\alpha k) + \frac{im}{\hbar}\{\varepsilon_{nk}-\varepsilon_{mk}\}\sum_{\alpha,\alpha'} c^*_{n\alpha'}(k)c_{m\alpha}(k)d_{\alpha'\alpha}. \tag{7}$$

The neglect of the second term in Eq. (7) reproduces Eq. (5).

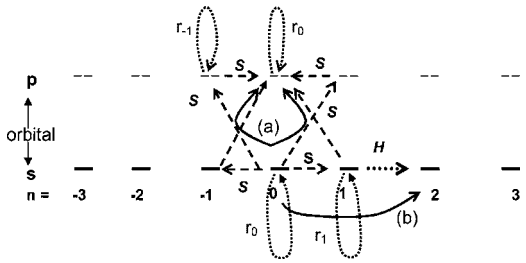

FIG. 1. (a) Schematic representation of the intra-atomic matrix elements of the coordinate operator induced by the orbital overlap; the generic model has two orbitals per site, *s*-like (solid lines) orbitals and *p*-like (dashed lines) orbitals. We illustrate the matrix elements r of the coordinate operator in the orthogonal basis by small dashed arrows, the overlap matrix elements S by dashed arrows, the matrix elements d of the coordinate operator in nonorthogonal basis by solid arrows, and the Hamiltonian matrix elements H in the nonorthogonal basis by dotted arrows. (b) Schematic representation of the increase in the range of the Hamiltonian in the orthogonalized basis by using the first order approximation in Eq. (10). The long-range matrix element of the Hamiltonian in the orthogonal basis connecting site 0 with site 2 for a nearest-neighbor Hamiltonian is shown by full arrow.

Therefore in the tight-binding basis, which is finite, by using Eq. (5) one is neglecting the second term in Eq. (7) or the intra-atomic part.[15] This shortcoming happens because the momentum and position operators do not satisfy the canonical commutation relations in a finite basis.[15] One way to add intra-atomic terms is the construction of Foreman.[16] However, intra-atomic terms can be induced if one considers a non-orthogonal basis. To show this, let us have an atomic basis with nonzero overlapping

$$(\chi_{\alpha R}|\chi_{\alpha' R'}) = 1 + S_{\alpha\alpha' RR'} = 1 + \mathrm{S}. \tag{8}$$

The orthogonal basis corresponding to Eq. (8) is (the Löwdin procedure)

$$|\chi') = (1+\mathrm{S})^{-1/2}|\chi). \tag{9}$$

In the orthogonal basis an operator transforms according to

$$A' = (1+S)^{-1/2}A(1+S)^{-1/2}. \tag{10}$$

Formally, expanding Eq. (9) in power series of S we rewrite Eq. (10) as

$$A' = A - \tfrac{1}{2}(SA+AS) + \tfrac{3}{8}(ASS+SSA) + \tfrac{1}{4}SAS\ldots. \tag{11}$$

The inverse transform of Eq. (10) has the following expansion:

$$A = A' + \tfrac{1}{2}(SA'+A'S) - \tfrac{1}{8}(A'SS+SSA') + \tfrac{1}{4}SA'S\ldots. \tag{12}$$

Now suppose that in the Löwdin basis the intra-atomic matrix element $d_{\alpha\alpha'}$ is zero, such that the Hamiltonian fulfills the gauge invariance conditions. In the original nonorthogonal (atomic) basis, however, there are intra-atomic elements. These can be easily seen if one applies the inverse transform Eq. (12) [Fig. 1(a)]. Thus in the atomic basis, up to the second order in S, the intra-atomic matrix element is

$$d_{R\alpha R\alpha'} = \frac{1}{8}\sum_{R''\alpha''} (-r_R S_{R\alpha',R''\alpha''}S_{R''\alpha'',R\alpha} - S_{R\alpha',R''}S_{R''\alpha'',R\alpha}r_R + 2S_{R\alpha',R''\alpha''}r_{R''}S_{R''\alpha'',R\alpha}). \quad (13)$$

Equation (13) shows us that in the atomic basis the intra-atomic matrix elements of coordinate operator are nonzero. Hence, considering the overlap, intra-atomic optical transitions can be incorporated. Although the intra-atomic corrections are second order in the overlap S, the overall corrections to the optical matrix elements are first order in S. In the same time the range of the Hamiltonian has been increased by applying the transformation given by Eq. (11) to the Hamiltonian matrix [Fig. 1(b)]. This result suggests that although a nearest-neighbor Hamiltonian might give a good reproducibility of the electronic structure, it completely misses the intra-atomic terms of optical matrix elements. The relationship between the overlap and longer ranged Hamiltonians is able to explain the nearest-neighbor spin-orbit interaction introduced in Ref. 19 in order to reproduce the Dresselhaus terms in zinc blend structures. Thus, the spin orbit contribution to the optical matrix elements, $\nabla_k H_{SO}(k)$, is nonzero. In the same time the initial prescription given by Chadi[20] is preserved. The overlap and long-range Hamiltonians are also closely interrelated in quantum wire transport. Using nearest-neighbor Hamiltonians, the overlap is crucial in explaining antiresonances in quantum wires.[25] However, the same antiresonances are reproduced with a Hamiltonian in which the effect of overlapping has been transferred to the second nearest-neighbor hoping elements.[26]

In a recent paper[21] it is shown that a piece-wise constant coordinate operator (and therefore diagonal) in *ab initio* TB-LMTO methods is analogous to the coordinate operator in semi-empirical methods. The most localized representation (TB representation), where the Hamiltonian is short ranged, is not the best for calculations although it is advantageous for numerical treatments. On the contrary, the coordinate operator was considered diagonal in the (nearly) orthogonal representation (with a long-ranged Hamiltonian) and used in transport calculations. The results were in very good agreement with the experimental values and with the results with the exact evaluation of the coordinate operator. Thus nonorthogonality plays an important role not only in empirical models but also in first-principles methods. If one assumes that the coordinate operator is piecewise constant and that the assumption is good enough, the calculations of the optical matrix elements can be obtained faster from electron band calculations. From Eq. (7), the k derivative of the Hamiltonian is calculated by fast Fourier transformations. Thus it is more computationally efficient than the usual scheme presented in Ref. 27. However, the applicability of a piecewise constant coordinate to optical properties of various physical systems remains to be investigated.

III. OPTICAL MATRIX ELEMENTS IN SIMPLE TIGHT-BINDING MODELS WITH OVERLAP

In the following we analyze the one-dimensional monoatomic crystal with two orbitals per atom, the one-dimensional diatomic crystal with one orbital per atom, and the two-dimensional graphene.

A. Monoatomic chain with two orbitals per atom

Schematic representation of a monoatomic chain with two orbitals per atom is given in Fig. 1. In a Bloch basis constructed from the overlapping orbitals, the nearest-neighbor tight-binding Hamiltonian for a monoatomic chain with two orbitals per site is a 2×2 matrix

$$H(k) = \begin{bmatrix} E_S + 2V_{SS}\cos(kL) & 2iV_{SP}\sin(kL) \\ -2iV_{SP}\sin(kL) & E_P + 2V_{PP}\cos(kL) \end{bmatrix}, \quad (14)$$

where E_S and E_P are the energies of s-like and p-like orbitals, respectively, V_{SS} and V_{PP} are the coupling of two nearest neighbor s-like and p-like orbitals, respectively, and V_{SP} is the coupling of a s-like orbital with the nearest neighbor p-like orbital. L is the length of the unit cell and k is the wave vector. The overlap matrix has a similar form

$$S(k) = \begin{bmatrix} 1 + 2S_{SS}\cos(kL) & 2iS_{SP}\sin(kL) \\ -2iS_{SP}\sin(kL) & 1 + 2S_{PP}\cos(kL) \end{bmatrix}. \quad (15)$$

In the orthogonal basis constructed according to Eq. (9), the Hamiltonian matrix $\tilde{H}$ is given by Eq. (10). The electronic bands are given by solving the eigenvalue problem $\tilde{H}(k)|nk\rangle = E_{nk}|nk\rangle$ and the interband matrix element of the kinematic momentum operator is $p(k) = m/\hbar\langle 1k|\tilde{H}'(k)|2k\rangle$, with $\tilde{H}'$ the derivative of $\tilde{H}$ with respect to k. We apply the above model to approximate the lowest two bands of the one-dimensional Kronig-Penney model. The Kronig-Penney model is a set of quantum wells of width a separated by barriers of height V_0 and width b. The case is investigated by Pedersen *et al.*[13] to suggest the need for intra-atomic contributions to optical transitions. We consider their strong-coupling case with $a=8$ Å, $b=1$ Å, and $V_0=5$ eV. The first state in the quantum well is an s-like state, while second state is a p-like state. Accordingly, in the tight-binding counterpart of the Kronig-Penney model, the overlap matrix elements S_{SP} and S_{PP} have to be negative. We adopt the same procedure[13] for fitting the energy bands of the Kronig-Penney model. The absolute values of the overlap matrix elements are chosen to be the same for S_{SS}, S_{SP}, and S_{PP}. The results are shown in Fig. 2 for an overlap of 0, 0.03, and 0.05 in comparison with the exact results of the Kronig-Penney model. While the energy bands are indistinguishable for tight-binding counterparts and agree well with the exact values, the interband momentum matrix elements vary and move toward exact values of the Kronig-Penney model. Because the absorption spectra are determined by the square modulus of the momentum matrix elements the above result is quite remarkable in the following sense as we explain below. Although we considered the strong coupling case (thin barriers), the coupling between s-like and p-like states is weak (the matrix element V_{SP} is an order of magnitude smaller than the other matrix elements) such that the electron bands have almost either s-like or p-like character over the entire Brillouin zone. Therefore, V_{SP} determines the magni-

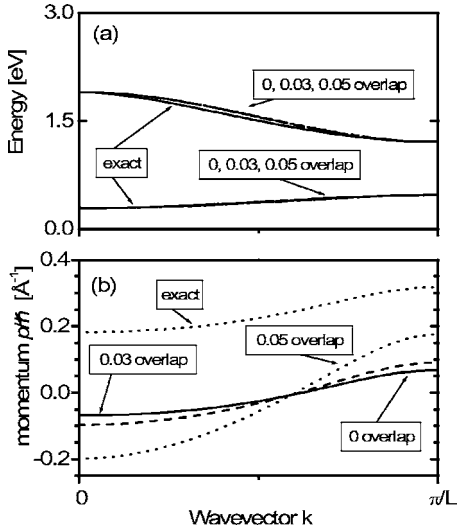

FIG. 2. (a) Band structure of the exact Kroning-Penney model and its approximations with a tight-binding model with overlap (see the text). Notice that following the same fitting procedure, the approximate bands are indistinguishable. (b) Momentum matrix elements of the exact Kroning-Penney model and its approximations with a tight-binding model with overlap. Notice the large variation of the momentum matrix elements with respect to the overlap while the bands are almost identical.

tude of the interband momentum matrix element. In the same time the validity of $p(k)=m/\hbar\langle 1k|\tilde{H}'(k)|2k\rangle$ is appropriate for strong interatomic coupling, such that the nearest-neighbor tight-binding model with orthogonal orbitals is inappropriate to calculate optical properties for the above model. Finally, we want to mention that in one-dimensional crystals with inversion symmetry the coordinate operator is diagonal in the basis generated by the Wannier functions.[28] Hence, the "closer" to the Wannier functions are the Löwdin orbitals, the better reproduced are the momentum matrix elements.

B. One-dimensional diatomic crystal with one orbital per atom

The chain is represented by s-like orbitals at positions nL and p-like orbitals at $nL+L/2$, where L is length of unit cell and n is integer. The interaction up to the second-nearest neighbor is illustrated in Fig. 3. The corresponding Hamiltonian matrix is

$$H=\begin{bmatrix} E_S+2V_{SS}\cos(kL) & 2iV_{SP}\sin(kL/2) \\ -2iV_{SP}\sin(kL/2) & E_P+2V_{PP}\cos(kL) \end{bmatrix}. \quad (16)$$

Similar form holds for the overlap matrix. This can be an approximate model for superlattices of type II, such as InAs-GaSB. In the InAs-GaSB superlattice the central feature is that the top of the GaSb valence band lies higher in energy than the bottom of the InAs conduction band, such that the electron and hole wave functions are overlapping. The electron/hole wave function is modeled by s-like/p-like orbitals. Keeping only the nearest neighbor interaction and overlap, the effect of overlapping is to decrease the momentum matrix elements as it is shown in Fig. 4. This simple

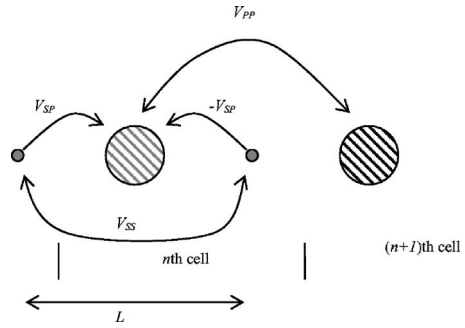

FIG. 3. Schematic representation of the diatomic linear chain with one orbital per atom and lattice constant L. The first type of atoms is depicted as small and full circles and the second type as stripped circles. The interactions between atoms are shown by arrows.

result might help in explaining the increase of the photoluminescence intensity with the reduction of the electron-hole wave function overlap,[29] which is not explained by the empirical pseudopotential calculations used to for this purpose.[30] The empirical pseudopotential method[30] used is nonatomistic, i.e., in their approach the Hamiltonian of the InAs/GaSb superlattice is constructed from the potential form factors of the InAs and GaSb bulk constituents. The potentials of the two bulk constituents are matched continuously at the interfaces such that there are no In-Sb or Ga-As bonds at the interface as there must be. As pointed out in Ref. 31 an atomistic description is desired to take into account charge redistribution, segregation, and interdiffusion at the interface between InAs and GaSb. In contrast to Ref. 30, Magri and Zunger[31] solve the single-particle Schrödinger equation for each atom in the structure making their method

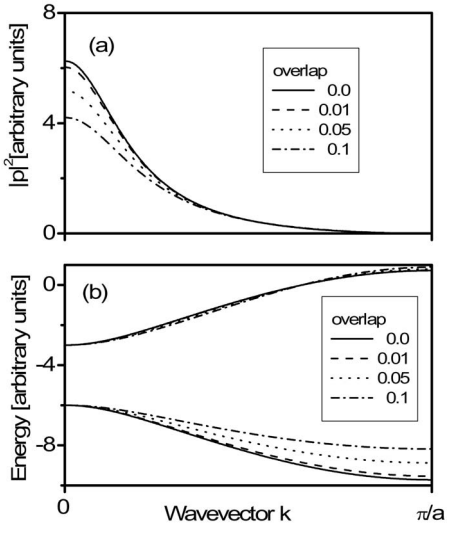

FIG. 4. (a) Optical matrix elements of the tight-binding model with overlap for a diatomic linear chain with one orbital per atom. (b) Energy bands of the tight-binding model with overlap for a diatomic linear chain with one orbital per atom. Full line is for 0 overlap, dash line for a 0.01 overlap, dot line for a 0.05 overlap, and dash-dot line for a 0.1 overlap. We choose arbitrary units because the system is rather generic.

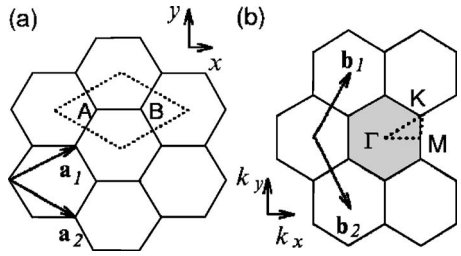

FIG. 5. (a) The unit cell of two-dimensional graphite is shown as the dotted rhombus. (b) The Brillouin zone of two-dimensional graphite is shown as the shaded hexagon. $\mathbf{a}_i$, and $\mathbf{b}_i$, $(i=1;2)$ are basis vectors and reciprocal lattice vectors, respectively. Energy dispersion relations and optical matrix elements are calculated along the perimeter of the dotted triangle connecting the high symmetry points, Γ, K, and M.

atomistic. In this sense, TB models preserve the atomistic description of interfaces.

C. Graphene

Recently, graphene as a two-dimensional sheet of graphite has been widely studied in the context of carbon nanotubes.[32] Graphite consists of a stack of graphene sheets piled up and weakly interacting one with each other. Graphene has a hexagonal structure with two atoms in the unit cell (Fig. 5) and very strong sp^2 bonds, causing a threefold coordinated planar structure. The remaining p_z orbitals are perpendicular to the plane, forming π (bonding) and π^* (antibonding) states. The overlap of π electrons with the intraplane sp^2 orbitals is small and π and π^* electronic states dominate the physical properties at low energy, around Fermi level. From Fig. 5 we easily deduce the nearest-neighbor tight-binding Hamiltonian and overlap matrix for π and π^* states as

$$H(k) = \begin{bmatrix} E_P & \gamma_0 f(k) \\ \gamma_0 f^*(k) & E_P \end{bmatrix} \tag{17}$$

and

$$S(k) = \begin{bmatrix} 1 & s_0 f(k) \\ s_0 f^*(k) & 1 \end{bmatrix}, \tag{18}$$

with $f(k)=e^{ik_y a/\sqrt{3}}+2e^{-ik_y a/2\sqrt{3}}\cos(k_x a/2)$, γ_0 is the nearest-neighbor transfer integral, E_p is the energy of π orbitals, s_0 is the nearest-neighbor overlap integral, a (=0.246 nm) is the lattice constant of graphite, and k is the two-dimensional wave vector. Experimental data or first principles calculations put γ_0 between 2.5 and 3 eV, $E_p=0$ eV, and s_0 is found to be below 0.1.[33] Due to their similar form, Hamiltonian matrix and overlap matrix have the same eigenvectors $|u^{\pm}\rangle = (1/2, \mp e^{-i\varphi}/2)$, with φ defined as $f(k)=|f(k)|e^{i\varphi(k)} = w(k)e^{i\varphi(k)}$. This yields the electronic eigenvalues

$$E^{\pm}(k) = \frac{E_p \mp \gamma_0 w(k)}{1 \mp s_0 w(k)}. \tag{19}$$

We note that the overlap makes the energy bands asymmetric with respect to the Fermi level and has large influence on bands. The full form of the Hamiltonian with overlap, $\tilde{H}$, is

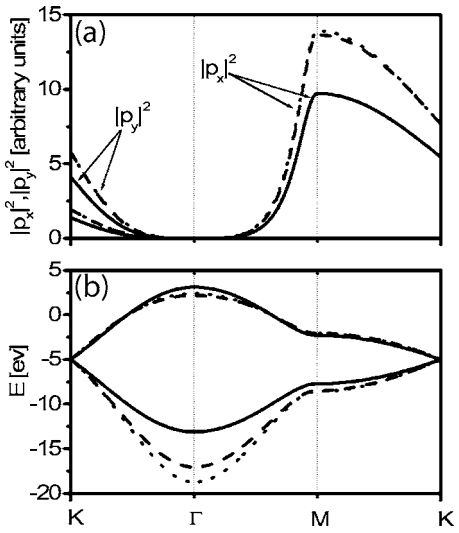

FIG. 6. (a) Optical matrix elements of the tight-binding model with overlap for the two-dimensional graphene. Since we are interested in the relative change of the momentum matrix elements with respect to overlap, arbitrary units are used. (b) Energy bands of the tight-binding model with overlap for the two-dimensional graphene. The values used are the following: $\gamma_0=2.7$ eV, $E_p=-5$ eV, and $s_0=0.1$. Full line is for $s_0=0$, dot line is for $s_0=0.1$, and dash line is for the first order approximation Hamiltonian [Eq. (12)] with $s_0=0.1$.

$$\tilde{H}(k) = \frac{1}{1-s_0^2 w^2(k)} \begin{bmatrix} E_P - s_0\gamma_0 w^2(k) & (\gamma_0 - s_0 E_p) f(k) \\ (\gamma_0 - s_0 E_P) f^*(k) & E_P - s_0\gamma_0 w^2(k) \end{bmatrix}. \tag{20}$$

Since s_0 is less than 0.1 we can safely discard the prefactor in Eq. (20). The diagonal part of the Hamiltonian matrix is proportional to the unit matrix in both cases, with or without overlap, and it does not contribute to the interband momentum matrix element. Therefore, one can easily calculate the intraband momentum matrix element in a compact form as

$$p = \frac{m}{\hbar}\langle u^+| \nabla \tilde{H}(k)|u^-\rangle = \frac{im}{\hbar}(\gamma_0 - E_p s_0)\frac{w(k)}{1-s_0^2 w^2(k)} \nabla \varphi(k). \tag{21}$$

Equation (21) shows us that for the most used parametrization ($E_p=0$ eV), the overlap does not play any role on the interband momentum since s_0 is less than 0.1 and we can safely discard the second order term is s_0. However, in order to fit the experimental dielectric function with the nearest-neighbor model, orbital overlapping is invoked in Ref. 34. It was found that $\gamma_0=2.7$ eV and $E_p=-5$ eV by assuming $s_0=0.1$. With this parameterization the numerical results are shown in Fig. 6 for the electronic bands and momentum matrix elements. The momentum matrix elements for the case with overlap are practically the same as those of the first order approximation Hamiltonian [Eq. (11)]. In the same time, the electronic bands generated by the first order Hamiltonian are different from those of the full Hamiltonian with overlap.

IV. CONCLUSIONS

We investigated the influence of the nonorthogonal orbitals on optical matrix elements in tight-binding models. A diagonal coordinate operator in the orthogonalized basis not only ensures the gauge invariance but also induces intraatomic contributions to the coordinate operator in the original (atomlike and nonorthogonal) basis. Moreover, the Hamiltonian matrix in the orthogonal basis is longer ranged than the Hamiltonian matrix in the initial nonorthogonal basis. As a consequence, one can justify the nearest-neighbor interaction of the spin-orbit coupling.[19] It enables to describe the Dresselhaus term, which is not considered in the usual treatment of the spin-orbit coupling.[20]

Simple models are analyzed. The first model studied was the monoatomic linear chain with two orbitals per site as an approximation to the Kronig-Penney model. The model was also used in Ref. 13 to show the role played by the intraatomic matrix elements of the momentum operator. We found that, although the tight-binding model with overlap exhibits almost the same energy bands as the one with orthogonal orbitals, the optical matrix elements are closer to the exact matrix elements of Kronig-Penney model. The second model studied was the biatomic linear chain with one orbital per site. This case showed that optical matrix elements decrease with overlap increasing. We also analyzed the optical matrix elements of the tight-binding model for two-dimensional graphite at low energies (between π and π^* electronic states). Optical matrix elements remain unchanged with respect to the overlap when the usual parametrization $E_P=0$ eV is adopted, while the bands change drastically. However, nonvanishing orbital overlapping and $E_P=-5.0$ eV are needed for better agreement with experimental data.[34]

In complete analogy with the above arguments, one can use a piecewise constant coordinate operator in the orthogonal representation of tight-binding linear muffin-tin orbitals methods[21] to calculate optical spectra from *ab initio*. The procedure will be faster because it will enable to calculate optical spectra directly from energy band calculations by employing the fast Fourier transformation and without directly evaluating the momentum operator.

ACKNOWLEDGMENT

The author wishes to acknowledge the support in part by the Office of Naval Research.

*Electronic address: tsandu@asu.edu

[1] *Tight-Binding Approach to Computational Materials Science*, edited by P. E. A. Turchi, A. Gonis, and L. Colombo (Materials Research Society, Warrendale, PA, 1998), Vol. 491.
[2] J. C. Slater and G. F. Koster, Phys. Rev. **94**, 1498 (1954).
[3] P.-O. Lowdin, J. Chem. Phys. **18**, 365 (1950).
[4] C. Delerue, M. Lannoo, and G. Allan, Phys. Status Solidi B **227**, 115 (2001).
[5] J. M. Jancu, R. Scholz, F. Beltram, and F. Bassani, Phys. Rev. B **57**, 6493 (1998).
[6] D. A. Papaconstantopoulos and M. J. Mehl, J. Phys.: Condens. Matter **15**, R413 (2003).
[7] T. B. Boykin, G. Klimeck, R. C. Bowen, and F. Oyafuso, Phys. Rev. B **66**, 125207 (2002).
[8] W. A. Harrison, *Elementary Electronic Structure* (World Scientific, River Edge, New Jersey, 1999).
[9] D. Nguyen-Manh, D. G. Pettifor, and V. Vitek, Phys. Rev. Lett. **85**, 4136 (2000).
[10] M. Graf and P. Vogl, Phys. Rev. B **51**, 4940 (1995).
[11] R. Peierls, Z. Phys. **80**, 763 (1933).
[12] M. Cruz, M. R. Beltran, C. Wang, J. Taguena-Martinez, and Y. G. Rubo, Phys. Rev. B **59**, 15381 (1999).
[13] T. G. Pedersen, K. Pedersen, and T. B. Kriestensen, Phys. Rev. B **63**, 201101(R) (2001).
[14] J. M. Jancu, A. Vasanelli, R. Magri, and P. Voisin, Phys. Rev. B **69**, 241303(R) (2004).
[15] T. B. Boykin and P. Vogl, Phys. Rev. B **65**, 035202 (2002).
[16] B. A. Foreman, Phys. Rev. B **66**, 165212 (2002).
[17] B. A. McKinnon and T. C. Choy, Phys. Rev. B **52**, 14531 (1995).
[18] D. A. Mirabella, C. M. Aldao, and R. R. Deza, Phys. Rev. B **50**, 12152 (1994).
[19] T. B. Boykin, Phys. Rev. B **57**, 1620 (1998).
[20] D. J. Chadi, Phys. Rev. B **16**, 790 (1977).
[21] I. Turek, J. Kudrnovsky, V. Drchal, L. Szunyogh, and P. Weinberger, Phys. Rev. B **65**, 125101 (2002).
[22] E. Blount, in *Solid State Physics*, edited by F. Seitz and D. Turnbull (Academic, New York, 1961), Vol. 13, p. 275.
[23] T. B. Boykin, Phys. Rev. B **52**, 16317 (1995).
[24] T. B. Boykin, R. C. Bowen, and G. Klimeck, Phys. Rev. B **63**, 245314 (2001).
[25] E. G. Emberly and G. Kirczenow, J. Phys.: Condens. Matter **11**, 6911 (1999).
[26] S. T. Rittenhouse and B. L. Johnson, Phys. Rev. B **71**, 035118 (2005).
[27] W. R. L. Lambrecht and S. N. Rashkeev, Phys. Status Solidi B **217**, 599 (2000).
[28] S. Kivelson, Phys. Rev. B **26**, 4269 (1983).
[29] A. P. Ongstad, R. Kaspi, C. E. Moeller, M. L. Tilton, D. M. Gianardi, J. R. Chavez, and G. C. Dente, J. Appl. Phys. **89**, 2185 (2001).
[30] G. C. Dente and M. L. Tilton, J. Appl. Phys. **86**, 1420 (1999).
[31] R. Magri and A. Zunger, Phys. Rev. B **68**, 155329 (2003).
[32] R. Saito, G. Dresselhaus, and M. S. Dresselhaus, *Physical Properties of Carbon Nanotubes* (Imperial, London, 1998).
[33] S. Reich, J. Maultzsch, C. Thomsen, and P. Ordejon, Phys. Rev. B **66**, 035412 (2002).
[34] T. G. Pedersen, Phys. Rev. B **68**, 245104 (2003).